

Finite Sections Modeling of Power Cable Systems

Luigi Colla, Stefano Lauria, Francesco Palone

Abstract-- The paper discusses the theoretical background and practical ATP-EMTP implementation of “Finite Sections” (FS) modeling of power cable systems. The model consists of cascaded multi-conductor “enhanced pi” cells where constant parameters, lumped R-L ladder networks reproduce current distribution within each conductor and in the ground; longitudinal coupling by lossless inductive arrays and appropriate R-C shunt networks complete an individual cell assembly, accounting also for dielectric losses and semi-conductive layers. Pipe/tunnel installation and earth stratification can also be included. The physical approach and analytical formulation for parameters calculation and circuit synthesis for single-core cables are detailed. ATP-EMTP circuit implementation as well as a routine for automatic calculation of circuit elements, model optimization and data case construction are also referred. Validation of the model versus the classic frequency dependent analytical solution is presented, showing a very good agreement in a frequency range from dc to 10 kHz and beyond.

Keywords: Cable modeling, transient analysis, ATP-EMTP, frequency dependence, finite sections.

I. INTRODUCTION

THE design of long cable systems to be installed in HV and EHV networks entails detailed transient and harmonic studies, in order to identify and address potential problem areas, some of which are uncommon in current transmission networks, mostly made of overhead lines [1] [2]. Accurate and reliable models are needed to this purpose [3]: however, while frequency-domain modeling is well established, time-domain simulation of power cables in the frequency range of interest to power system transients, i.e. from dc to 1 MHz still poses difficulties. Modal analysis techniques with constant transformation matrices [4], successfully applied to overhead lines, are less suited to underground cable systems on account of the strong frequency dependence of transformation matrices [5]. Other models accounting for frequency dependence of transformation matrices and based on fitting techniques [6],[7] may suffer numerical instability due to computation (truncation) errors, unstable poles fitting of the transfer matrix and interpolation errors on modal time delays that are not in general integer

multiples of the simulation time step in EMTP-like softwares. [5]. Numerical instability can occur especially in simulation of transients involving frequencies between dc and some kHz.

Transmission lines modeling by means of cascaded pi sections has been used since the 60ies with Transient Network Analyzers (TNAs). Criteria for pi sections unit length have been well defined, namely the line length has to be short compared with a quarter wavelength of the highest frequency being considered [8]. Dealing with cable systems this condition has to be verified for all the propagation modes of interest. The classical cascaded pi approach makes use of pi sections calculated at one frequency and therefore it does not take into account the frequency dependence of current distribution (skin effect) in conductors and ground.

This paper deals with the application and extension of the “Finite Sections” (FS) method proposed in [9], that is, cable modeling by means of cascaded lumped-parameter cells taking explicitly into account the frequency dependence of conductors and ground impedances. The result is a multi-conductor model, suitable for both time and frequency domain, made of lumped R-L-C elements and coupling transformers inductive arrays only, directly obtained by physical-geometrical data, ruling out non-passive realizations and numerical instability. The number of model elements can be increased to meet the required bandwidth and accuracy, which practically is not a limit for usual power system transient studies; dc operation and trapped charge do not pose problems. Features such as dielectric losses, semicon layers, ferromagnetic armour and pipe/tunnel installation are straightforwardly incorporated in the model.

This paper focuses on the background of the FS method and the validation of the individual building blocks of the model, against classic analytical treatments. Section II recalls the ladder circuit representation of cylindrical conductors, whereas section III recounts the extension of the approach to ground return modeling. Section IV explains the assembly of individual ladder networks into the “Enhanced pi” sections; model assembly is completed in Section V, where shunt circuits representing semi-conductive and dielectric media are detailed.

II. LADDER NETWORK REPRESENTATION OF CYLINDRICAL CONDUCTORS

R-L ladder (Cauer) networks have been long used in Transient Network Analyzers (TNAs) [8], to reproduce the frequency dependent behavior of transmission lines’ conductors and ground return paths. An analytical derivation of the network and its circuit elements from conductor characteristics is given e.g. in [10] and reported here.

S. Lauria is with the Dept. of Astronautics, Electrical and Energetics Engineering, University of Rome “Sapienza”, via Eudossiana 18, 00184 Rome, Italy (e-mail of corresponding author: stefano.luria@uniroma1.it).

L. Colla and F. Palone are with TERNA S.p.A., Grid Development and Engineering, via Galbani 70, 00156 Rome, Italy (e-mail luigi.colla@terna.it, francesco.palone@terna.it).

Neglecting the displacement currents inside a conductor, Maxwell 3rd and 4th equations can be written as follows:

$$\nabla \times \vec{J} = -\mu\sigma \frac{\partial \vec{H}}{\partial t}, \quad \nabla \times \vec{H} = \vec{J} \quad (1)$$

Moreover, considering radial symmetry and longitudinal (axial) current in a cylindrical conductor, the scalar differential relationship between current density $J(r,t)$ at radial distance r and enclosed current $I(r,t)$ is:

$$\frac{\partial J(r,t)}{\partial r} = \frac{\mu\sigma}{2\pi r} \frac{\partial I(r,t)}{\partial t} \quad (2)$$

This can be discretized by subdividing the conductor into concentric rings of constant current density, as shown in Fig.1. With the notations of Fig.1, (2) becomes:

$$\frac{J_{i-1} - J_i}{r_{i-1} - r_i} = \frac{\mu\sigma}{2\pi r_i} \frac{\partial I_i(r,t)}{\partial t} \quad (3)$$

If current density is considered constant between the radii r_{i-1} and r_i then

$$J_i = \frac{I_{i+1} - I_i}{A_i}, \quad A_i = \pi(r_{i+1}^2 - r_i^2) \quad (4)$$

Being I_i the current enclosed in the radius r_i , and A_i the area of the i -th layer. Thus, using (3) and (4):

$$R_{i-1}(I_{i-1} - I_i) - R_i(I_i - I_{i+1}) = L_i \frac{dI_i}{dt} \quad (5)$$

$$R_i = \frac{1}{A_i \sigma}; \quad L_i = \frac{\mu(r_{i+1} - r_i)}{2\pi r_i}$$

The former equations represent a rung of the Cauer ladder network of Fig. 1. Notably, as the layers' thickness decreases the L_i definition numerically converges to the one given by Meredith [1].

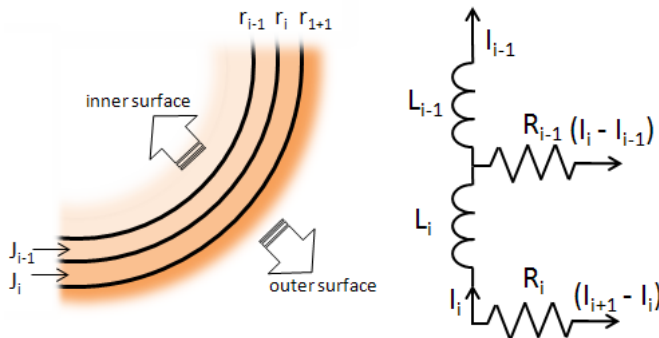


Fig. 1. Discretization of cylindrical conductor and corresponding equivalent ladder network representation (see text for details)

$$L_i = \lim_{r_i \rightarrow r_{i+1}} \frac{\mu}{2\pi} \ln\left(\frac{r_{i+1}}{r_i}\right) = \frac{\mu(r_{i+1} - r_i)}{2\pi r_i} \quad (6)$$

At dc, with nil inductive reactance, the current density is constant along the radius, whereas at increasing ac frequency the voltage drop along the inductance forces the current to flow near the external surface of the conductor.

Interestingly the current-to-voltage transfer function $Z(\omega)$ of the Cauer ladder network can be written as a continuous fraction (7), which for an infinite number of terms yields the

ratio between Bessel functions of the first kind, J_0/J_1 [11], i.e. the analytical formulation of the surface impedance for cylindrical conductors [12]. Furthermore (7) can be represented by a pole-residue expansion, yielding in turn an equivalent Foster network [13]. This polynomial representation of the conductor impedance, with its attendant equivalent circuit, directly descends from the discretization of Maxwell's equations without resorting to error minimization or fitting procedures.

$$Z(\omega) = \frac{1}{1 + \frac{1}{R_1 + \frac{1}{j\omega L_1 + \frac{1}{1 + \frac{1}{R_2 + \frac{1}{j\omega L_2 + \frac{1}{\frac{1}{R_3} + \frac{1}{j\omega L_3}}}}}}} \dots} \quad (7)$$

Every layer introduced in the conductor representation adds a zero-pole pair in the transfer function; as the circuit is made of $R-L$ lumped elements, it is physically impossible to generate unstable poles, so the stability of the model is ensured. It is evident that the thinner the layers, the wider the frequency window that can be represented by Finite Sections modeling for a given maximum error. To prove the effectiveness of this method a comparison has been made between analytical formulae [14] and the impedances as resulting from finite sections modeling.

At first, a small algorithm capable to generate ATP-EMTP data files containing the equivalent circuit of each conductor was made; the program includes a Genetic Algorithm (GA) subroutine for finding the optimal number and thicknesses of the conductor layers for a given target precision. This pre-processing operation is analogous to the meshing procedure in a Finite Elements Method simulation. The GA subroutine searches the parameters that yield the minimum error for a given number of layers (alternatively, the number of layers vs. allowable error). Even an arbitrary choice of layers number and thicknesses, however, does not inhibit the smooth functioning of the method, although more computational resources are needed to achieve the same precision.

In principle, analogously to what is reported in [8] for pi section length, a good criterion is to have layers' thicknesses small compared with penetration depth associated to the highest frequency being considered. It should be noted that deeper layers are not affected by higher frequency currents and can therefore be thicker than outer layers. For example, good results can be obtained using a geometrical progression of the layers' thicknesses [9].

The cable system chosen for validation and referred to throughout the paper, shown in Fig. 2, is usual in the Italian HV sub-transmission networks. Setting e.g. the maximum allowable error on the core conductor impedance at 10^{-4} p.u. in the $(10^3 \div 10^6)$ Hz range, the routine shows that 300 layers are required: Figs. 3 and 4 prove that using the Finite Sections method it is possible to obtain any reasonable accuracy in

conductor representation; on the other hand it is possible to reduce the computational burden by exchanging some precision with memory allocation and simulation speed.

Geometric data	
Conductor radius	24.5 mm
Inner semi-conductor width	2 mm
Insulation width	15.8 mm
Outer semi-conductor width	1.3 mm
Metallic sheath width	0.6 mm
Total diameter	100 mm
Typical laying data	
Laying distance (D)	200 mm
Laying depth (h)	1200 mm
Electric data	
DC resistance at 20°C	19 mΩ/km
Capacitance	300 nF/km

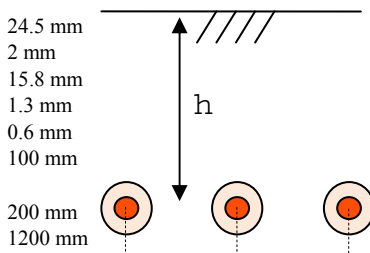


Fig. 2. Electrical and geometrical data of the sample 150 kV, 1600 mm² Al, XLPE-insulated underground cable system.

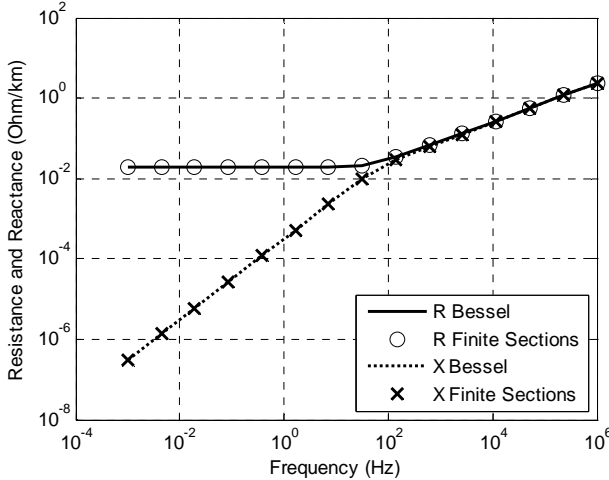


Fig. 3. 300-layers finite sections model and analytical expression of outer surface resistance and reactance (for 1km of length), for core conductor of Fig. 2 cable, vs. frequency.

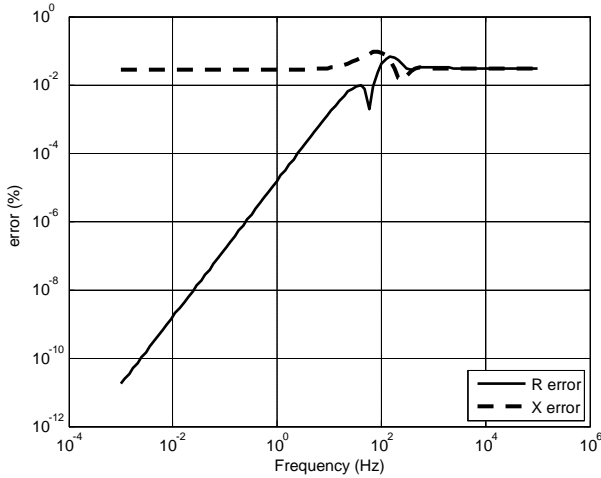


Fig. 4. Percent error of 300-layers finite sections outer surface resistance and reactance (see Fig. 3) vs. frequency.

Figs. 5 and 6 show that with 15 layers, a maximum impedance error below 1.4% and an average impedance error

of 0.25% are achieved in the range (10⁻³–10⁵) Hz. Such errors are still small if compared to all other uncertainties introduced in line modeling, so that even cable modeling by a relatively small network can be satisfactory for most harmonic and transient studies.

III. LADDER NETWORK REPRESENTATION OF THE EARTH RETURN PATH

The earth return path impedance is present in all terms of the longitudinal impedance matrix [15]; its analytical formulation involves the calculation of the Pollaczek infinite integral which is still a difficult numerical task even with the use of dedicated algorithms [16]. In most practical cases, however, it is not worthwhile to make such a complex analysis; the error introduced by replacing it with the Carson-based approximation [17] or with the well-established Wedepohl-Wilcox approximation [18], using formula (8), is low enough especially when compared to the uncertainties affecting parameters (e.g. resistivity) and geometry of the earth return path.

$$Z_E = \frac{\mu\omega\epsilon}{2\pi} \left\{ -\ln\left(\frac{rm\gamma}{2}\right) + \frac{1}{2} + \frac{4}{3}mh \right\} \quad (8)$$

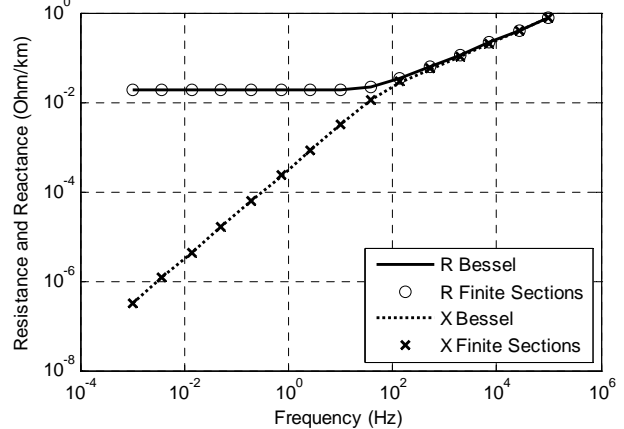


Fig. 5. 15-layers finite sections model and analytical expression of outer surface resistance and reactance (for 1km of length) for core conductor of Fig. 2 cable, vs. frequency.

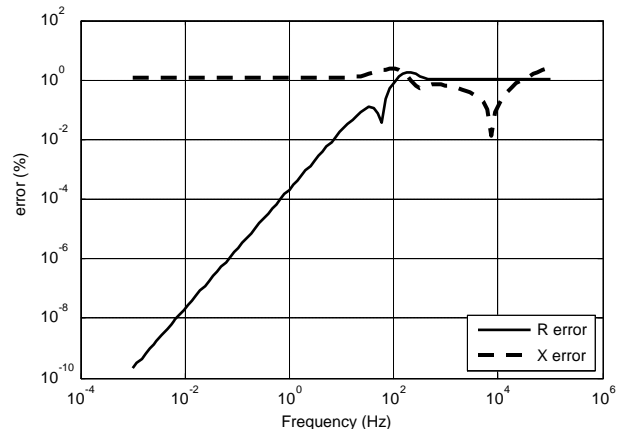


Fig. 6. Percent error of 15-layers finite sections outer surface resistance and reactance (see Fig. 5) vs. frequency.

FS modeling of a power cable system requires the representation of the earth return path as another coaxial cylindrical conductor, encircling all the cables of the system, with the soil resistivity value being twice the actual one [9]. Figs. 7 to 9, referring to a 75-layers ground representation, show that this simple approximation is actually quite satisfactory since it does not introduce large errors, although more layers are required in order to achieve the accuracy of other conductors' models. It must be also pointed out that for the earth return path it is not necessary to pursue high accuracy representation in the high frequency range, because the shielding effect of the metal sheaths and armour (if present) hinders the penetration of high frequency currents in the ground; the number of layers for earth return was accordingly chosen for a frequency range extending from dc to 10 kHz for the study case dealt within this paper.

Figs. 7 to 9 clearly show that the error introduced by FS modeling of the ground return path is negligible in the frequency range between 0 and 10 kHz, the more so considering the uncertainty surrounding ground resistivity. The frequency bandwidth could be easily enlarged by increasing the number of layers, weighting the attendant increase in computational burden against the actual relevance of ground conduction at frequencies above some kHz.

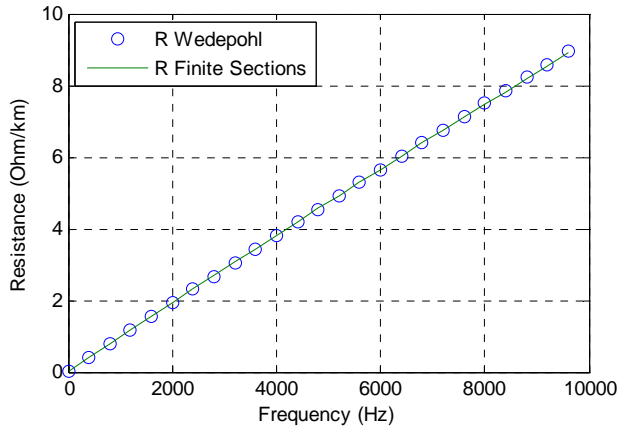


Fig. 7. Earth return resistance vs. frequency of Fig. 2 cable system ($100 \Omega\text{m}$ ground resistivity) for finite sections (75 layers) and Wedepohl-Wilcox formula.

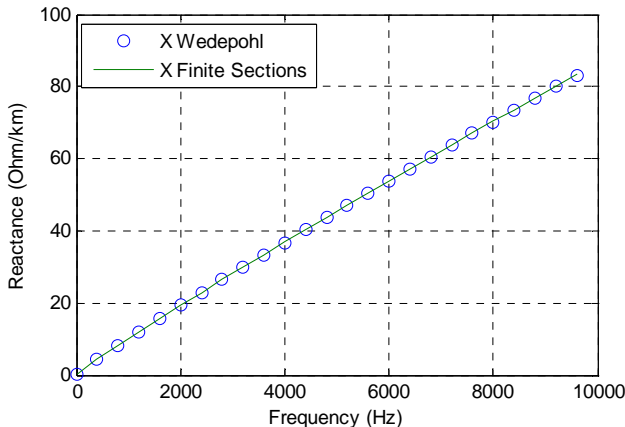


Fig. 8. Earth return reactance vs. frequency of Fig. 2 cable system ($100 \Omega\text{m}$ ground resistivity) for finite sections (75 layers) and Wedepohl-Wilcox formula.

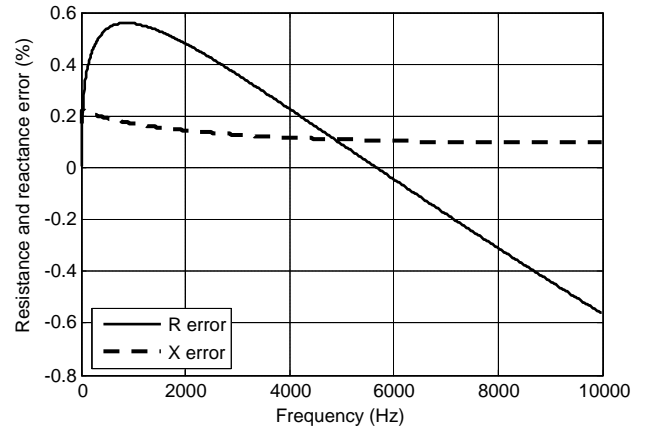


Fig. 9. Earth return path resistance and reactance (see Fig. 7 and 8) percent error vs. frequency, with respect to Wedepohl-Wilcox formula.

The GA subroutine described in Section II also applies to earth return modeling; generally speaking, a simple criterion might be to represent ground layers starting at some meters from the cable system down to about 10 times the penetration depth in the soil, calculated at the lowest frequency involved in the study. Even in dc studies it is actually sufficient to stop modeling when the longitudinal resistance of ground layers becomes negligible if compared with “local” earthing (electrode) resistance. Soil stratification can be straightforwardly included in finite sections modeling by just setting different values of resistivity for different layers of the ground return path, as well as changing such values along the cable route, from one longitudinal circuit block to the other. Although in most practical cases geophysical data are not available and uniform earth path is considered, this capability is useful to properly represent tunnel/pipe installation without any change in the model structure.

IV. CIRCUIT SYNTHESIS

Ladder networks obtained from FS modeling of individual conductors must be combined in an enhanced pi section, in order to model a cable system. Several enhanced pi sections must be cascaded according to the criterion recalled in [8]. Two cascaded sections of the assembled “enhanced pi” circuit are shown in Fig. 10 [9] for a single coaxial cable with conductor core, metallic sheath and armour; the equivalent ground ladder network is also included. In the usual series impedance formulation [17], the ground is not explicitly represented as a conductor, and ground return impedance is instead embedded into conductors’ self-impedance and mutual impedance terms. In this way voltages to ground, i.e. the voltage differences between conductors and local ground, are correctly obtained at any location along the line, the only lost information being the local ground voltage (with respect to remote earth).

Since FS modeling relies instead on physical representation of every conductor including the ground, only one point can be taken as reference. The ground surface at one “enhanced pi” terminal, i.e. the inner layer of the equivalent earth, must

be chosen as the reference for the zero voltage; thus conductor voltage to local earth surface coincides with the voltage to ground found with the classical representation.

Lumped resistances, marked “G mat” in Fig. 10 stand for actual earthing resistances at grounding points (such as substation ground mats, sheath earthing points...), where current can actually flow into and out of the ground.

For a correct synthesis of the cable system impedance matrix, as given e.g. in [17], coupling transformers [9] must be used in each enhanced pi section to allow the explicit allocation of internal conductor inductances to the physically distinct circuits pertaining to those conductors. This could be verified by checking the equivalent circuit of Fig. 10 for any self-impedance term in the standard Ametani formulation, most notably the “core” term Z_{cc} which contains all individual “conductor” impedance terms [15].

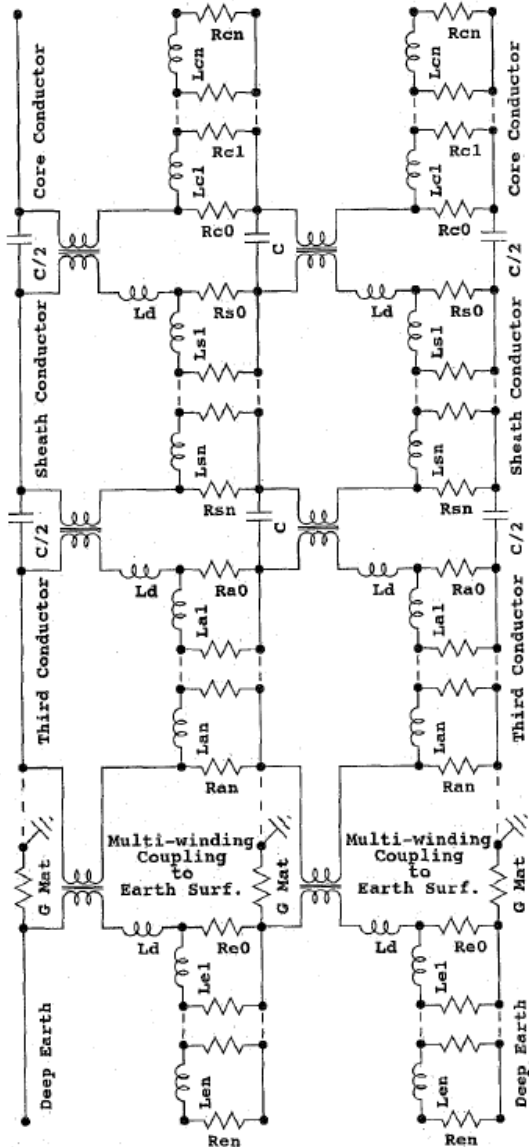


Fig. 10. Meredith's [9] “enhanced pi” circuit for finite section modeling of multiple coaxial conductors, including earth.

The quasi-ideal transformers of Fig. 10 notably allow to reproduce the shielding action of outer tubular conductors even if the latter are not injected with current. The practical ATP-EMTP representation of coupling transformers implies the use of Type 51-52-53 [19] impedance matrices, instead of the ideal transformer component (that contains an internal voltage source connected to the remote earth); Type 51-52-53 must in turn account for a large magnetizing term in order to preserve near-ideal coupling, yet not so large to cause numerical errors. When only metallic conductors (core, sheath, armour) are involved, the leakage impedance L_d of coupling transformers coincides with the external impedance of the coaxial system (core-to-sheath or sheath-to-armour). When considering the inductive coupling between outer conductor and earth, two issues arise:

- firstly, circuit modeling of the earth surrounding the cable system must begin at some distance from the cables (few meters are sufficient) in order to preserve the cylindrical symmetry hypothesis;
- secondly, for a multi-cable system, mutual coupling between all the outer conductors has to be represented.

The adoption of a further leakage term, accounting for the distance between outer cable surface and inner “equivalent earth” surface, solves the first issue. The second issue is addressed by the multi-winding transformers shown in Fig. 10, noting that the correct representation of the mutual impedance between conductors belonging to different cables [15] requires to take into account the leakage impedance between outer cable conductors as well as between each of these and the inner earth surface.

Figs. 11 and 12 show the comparison between FS modeling (respectively using 300, 25 and 75 layers for core conductor, metallic sheath and ground) and reference solution [15] for the Z_{cc} term. By comparing Fig. 12 with Figs. 4 and 9 it can be noted that the ground return is the most important part for model precision; as pointed out in Sec. III, the relevance of earth-related terms decreases beyond a few kHz. In the considered frequency interval, however, the series impedance of the cable system is correctly reproduced.

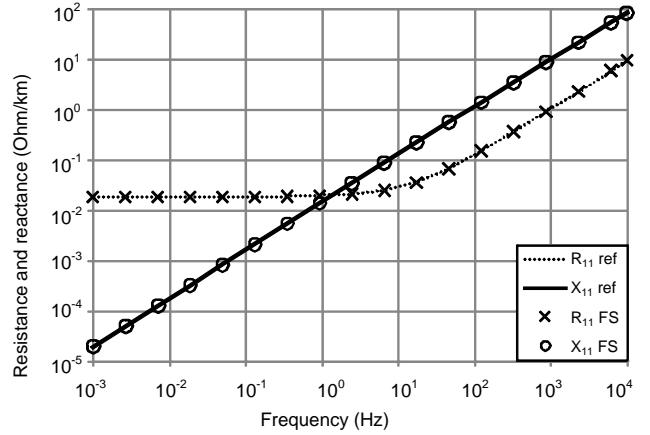


Fig. 11. Z_{cc} (core conductor) longitudinal impedance vs. frequency, for 1km of length of Fig. 2 cable. Finite sections model and reference solution in real and imaginary part (see text for details).

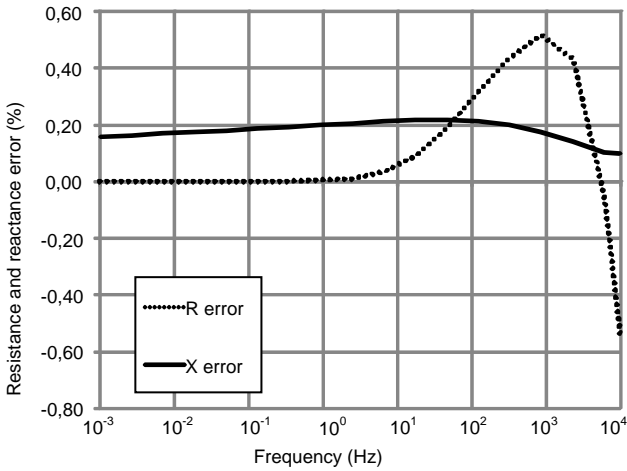


Fig. 12. Error of finite sections Z_{cc} longitudinal impedance, in real and imaginary part, with respect to reference solution, vs. frequency, (see Fig. 11).

V. MODELING OF INSULATION AND SEMI-CONDUCTIVE LAYERS

The model is completed by the inclusion of shunt branches, taking into account capacitance and dielectric losses. Capacitive elements in Fig. 10 are straightforwardly obtained by the cable system capacitance matrix, calculated for the length of the individual “enhanced pi” section. Capacitive elements are simply connected between the external layer of the inner conductor and the internal layer of the outer conductor. Furthermore, due to the strong frequency dependence of the conductor-sheath conductance and its primary role in high frequency wave attenuation, it is important to include it in a wideband model, by replacing the relevant lumped capacitance with a small R-C (Foster) network similar to [20][21]. Fig. 13a shows the proposed equivalent shunt circuit representing the cable insulation. Parameters of the proposed circuits have been obtained by matching three values of (complex) shunt admittance for three different frequencies; Fig. 13b represents the conductance and susceptance for constant $\tan(\delta)$ (dielectric loss factor) hypothesis and the circuit admittance versus frequency.

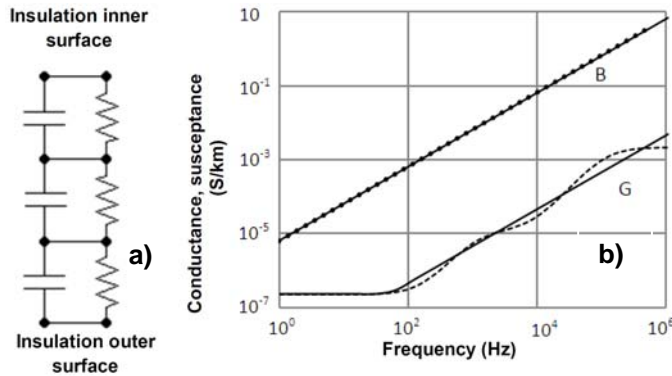


Fig. 13. a) Proposed 6-elements circuit for lossy insulation and semiconductor representation. b) Equivalent shunt parameters of main insulation (B: susceptance; G: conductance) vs. frequency for constant $\tan(\delta)$. Theoretical (continuous line) and calculated (dashed line) values.

The simple model gives a satisfactory fitting in the frequency range of interest; furthermore different insulation behaviors (e.g. paper-oil cables with non-constant loss factor [22]) can be represented. It is also possible to take into account straightforwardly semi-conductive layers by adding appropriate R-C cells in series with the main insulation equivalent circuit. An additional advantage of this explicit representation of dielectric media is the effective damping of Gibbs oscillations inherent to the lumped parameters circuit.

VI. CONCLUSIONS

The paper presented the theoretical background and a step-by-step validation of the “finite sections” technique leading to a general, multi-conductor wideband model for both time and frequency domain simulation of power cables in EMTP softwares. The method, conceptually based on discrete integration of Maxwell’s equations, can be summarized as the longitudinal discretization of the cable line into a cascade of “enhanced-pi” circuits consisting only of lumped R-L-C elements, which take explicitly into account the frequency dependent current distribution within conductors and ground, from dc to several hundreds of kHz. In addition to the original model [9], also the frequency dependence of cables shunt parameters (notably dielectric losses) can be taken into account.

The strong physical meaning of the FS approach allows to directly obtain the cable model from physical-geometrical data. Mathematical fitting of impedance functions is not involved. Model validation by comparison with analytical expression of longitudinal impedance matrix elements showed very good results. The model is inherently rugged from a numerical point of view; the computational burden is nevertheless fully within the present-day capability of personal computers and EMTP softwares. Moreover the tasks related to model building and assembling are taken care of by an automatic routine developed by the authors. The intrinsic numerical stability of the model as well as its accuracy in the frequency range of interest to power system transients point out to a wide range of applications in power systems analysis.

The above properties prompted the use of a FS-based cable model for the preliminary transient study of an international HVDC link planned by TERNA S.p.A. [23].

Short term developments include modeling of three-core and pipe-type cables as well as inclusion of ferromagnetic armour [24].

VII. REFERENCES

- [1] L. Colla, F. M. Gatta, F. Iliceto, and S. Lauria, "Design and operation of EHV transmission lines including long insulated cable and overhead sections," in *Proc. 2005 IEEE International Power Engineering Conference*, Singapore, 2005.
- [2] M. Rebolini, L. Colla, F. Iliceto "400 kV AC new submarine cable links between Sicily and the Italian mainland. Outline of project and special electrical studies," in *Proc. CIGRE 2008*, Paris, Aug. 2008.

- [3] B. Gustavsen, J. A. Martinez, and D. Durbak, "Parameter determination for modeling system transients—Part II: insulated cables," *IEEE Trans. Power Delivery*, vol. 20, pp. 2045-2050, Jul. 2005.
- [4] J. R. Marti, "Accurate modelling of frequency-dependent transmission lines in electromagnetic transient simulations," *IEEE Trans. Power Apparatus and Systems*, Vol. 101, pp. 147-157, Jan. 1982.
- [5] I. Kocar, J. Mahseredjian, and G. Olivier, "Improvement of numerical stability for the computation of transients in lines and cables," *IEEE Trans. Power Delivery*, vol. 25, pp. 1104-1111, Apr. 2010.
- [6] L. Marti, "Simulation of transients in underground cables with frequency-dependent modal transformation matrices," *IEEE Trans. Power Delivery*, vol. 11, pp. 1099–1110, Jul. 1988.
- [7] A. Morched, B. Gustavsen, and M. Tartibi, "A universal model for accurate calculation of electromagnetic transients on overhead lines and underground cables," *IEEE Trans. Power Delivery*, vol. 14, pp. 1032–1038, Jul. 1999.
- [8] A. Greenwood, *Electrical Transients in Power Systems*, 2nd edition. New York: Wiley, 1991, p. 365.
- [9] R. J. Meredith, "EMTP Modelling of electromagnetic transients in multi-mode coaxial cables by finite sections," *IEEE Trans. Power Delivery*, vol. 12, pp. 489-497, Jan. 1997.
- [10] C. Yen, Z. Fazarinc, and R. L. Wheeler, "Time domain skin effect model for transient analysis of lossy transmission lines," *Proceedings of the IEEE*, vol. 70, pp. 750-759, July 1982.
- [11] P. Flajolet and R. Schott, "Non overlapping partitions, continued fractions, Bessel functions and a divergent series," *European Journal of Combinatorics*, vol. 11, pp. 412-432, 1990.
- [12] G. Bianchi and G. Luoni, "Induced currents and losses in single-core submarine cables," *IEEE Trans. Power Apparatus and Systems*, vol. 95, pp. 49-58, Jan. 1976.
- [13] K. Murthy and R. Bedford, "Transformation between Foster and Cauer equivalent networks," *IEEE Trans. Circuits and Systems*, vol. 25, pp. 238-239, Apr. 1978.
- [14] S. A. Schelkunoff, "The electromagnetic theory of coaxial transmission line and cylindrical shields," *Bell Syst. Tech. J.*, vol. 13, pp. 532–579, 1934.
- [15] H. Domme, "EMTP Theory Book," Bonneville Power Administration, Portland, OR, Aug. 1986.
- [16] F. A. Uribe, J. L. Naredo, P. Moreno, and L. Guardado, "Algorithmic Evaluation of Underground Cable Earth Impedances," *IEEE Trans. Power Delivery*, vol. 19, pp. 316-322, Jan. 2004.
- [17] A. Ametani, "A general formulation of impedance and admittance of cables," *IEEE Trans. Power Apparatus and Systems*, vol. 99, pp. 902–910, May 1980.
- [18] L. M. Wedepohl and D. J. Wilcox, "Transient analysis of underground power-transmission system - system model and wave propagation characteristics," *Proceedings of IEE*, vol. 120, pp. 253–260, Feb. 1973.
- [19] Canadian-American EMTP Users Group, "ATP-EMTP Rule Book, 1997.
- [20] G. C. Stone and S. A. Boggs, "Propagation of partial discharge pulses in shielded power cables," in *Proc. Conf. Electric Insulation and Dielectric Phenomena*, pp. 275-280, Washington, D.C., Oct. 1982.
- [21] J. J. Guo, L. Zhang, C. Xu, and S. A. Boggs, "High Frequency Attenuation in Transmission Class Solid Dielectric Cable," *IEEE Trans. Power Delivery*, vol. 23, pp. 1713-1719, Oct. 2008.
- [22] O. Breien and I. Johansen, "Attenuation of traveling waves in single-phase high-voltage cables," *Proceedings of IEE*, vol. 118, pp. 787–793, Jun. 1971.
- [23] L. Colla, S. Lauria, and F. Palone, "HVDC-VSC Short Circuit Calculation," in *Proc. 2010 EEUG Meeting*, Helsinki (Finland), Aug. 2010.
- [24] M. Popov, L. Grcev, L. van der Sluis, and V. V. Terzija, "An ATP-EMTP-based model for analysis of shielding properties of ferromagnetic cable sheaths," *IEEE Trans. Power Delivery*, vol. 20, pp. 2241-2247, Jul. 2005.